

Supplementary Information

Sn₄P₃-C nanospheres as high capacitive and ultra-stable anodes for sodium ion and lithium ion batteries

*Jonghyun Choi, Won-Sik Kim, Kyeong-Ho Kim, and Seong-Hyeon Hong**

Department of Materials Science and Engineering and Research Institute of Advanced
Materials, Seoul National University, Seoul 151-744, Republic of Korea

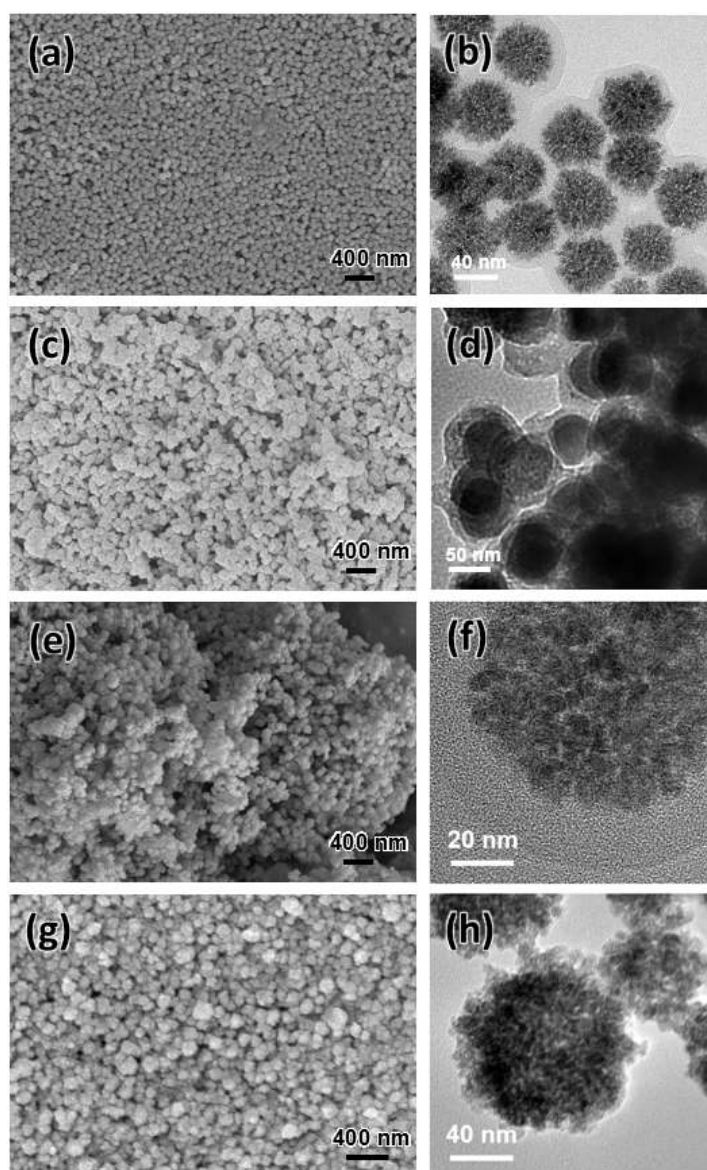
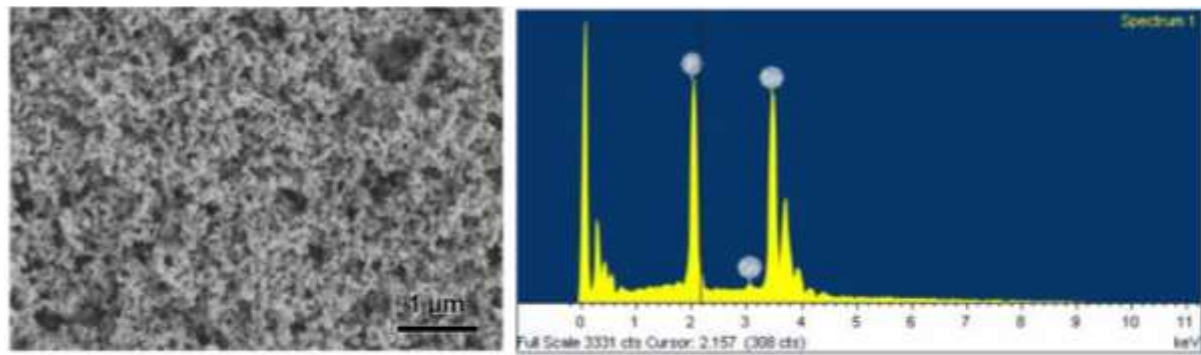


Fig. S1 SEM and TEM images of nanospheres: (a),(b) SnO₂-GCP, (c),(d) Sn-C, (e),(f) Sn₄P₃-C, and (g),(h) Sn₄P₃ nanospheres.



Element	Weight %	Atomic %
Sn	84.28	58.32
P	15.72	41.68

Fig. S2 EDS results for the $\text{Sn}_4\text{P}_3\text{-C}$ nanospheres.

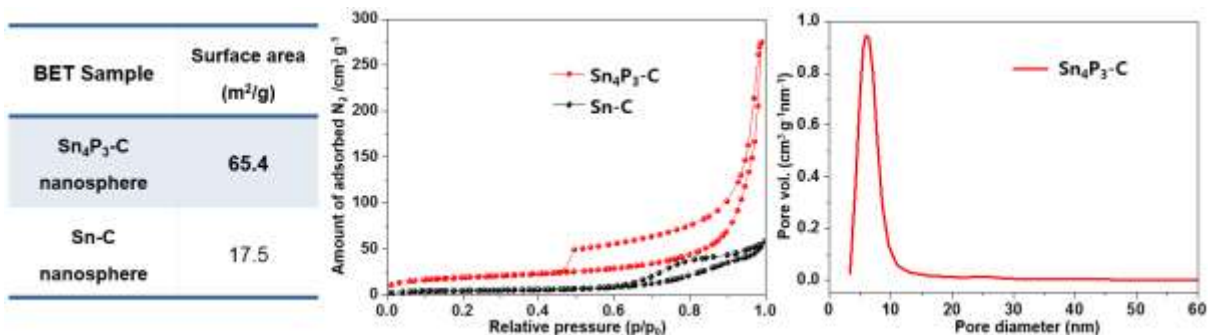


Fig. S3 BET results for the Sn-C and $\text{Sn}_4\text{P}_3\text{-C}$ nanospheres.

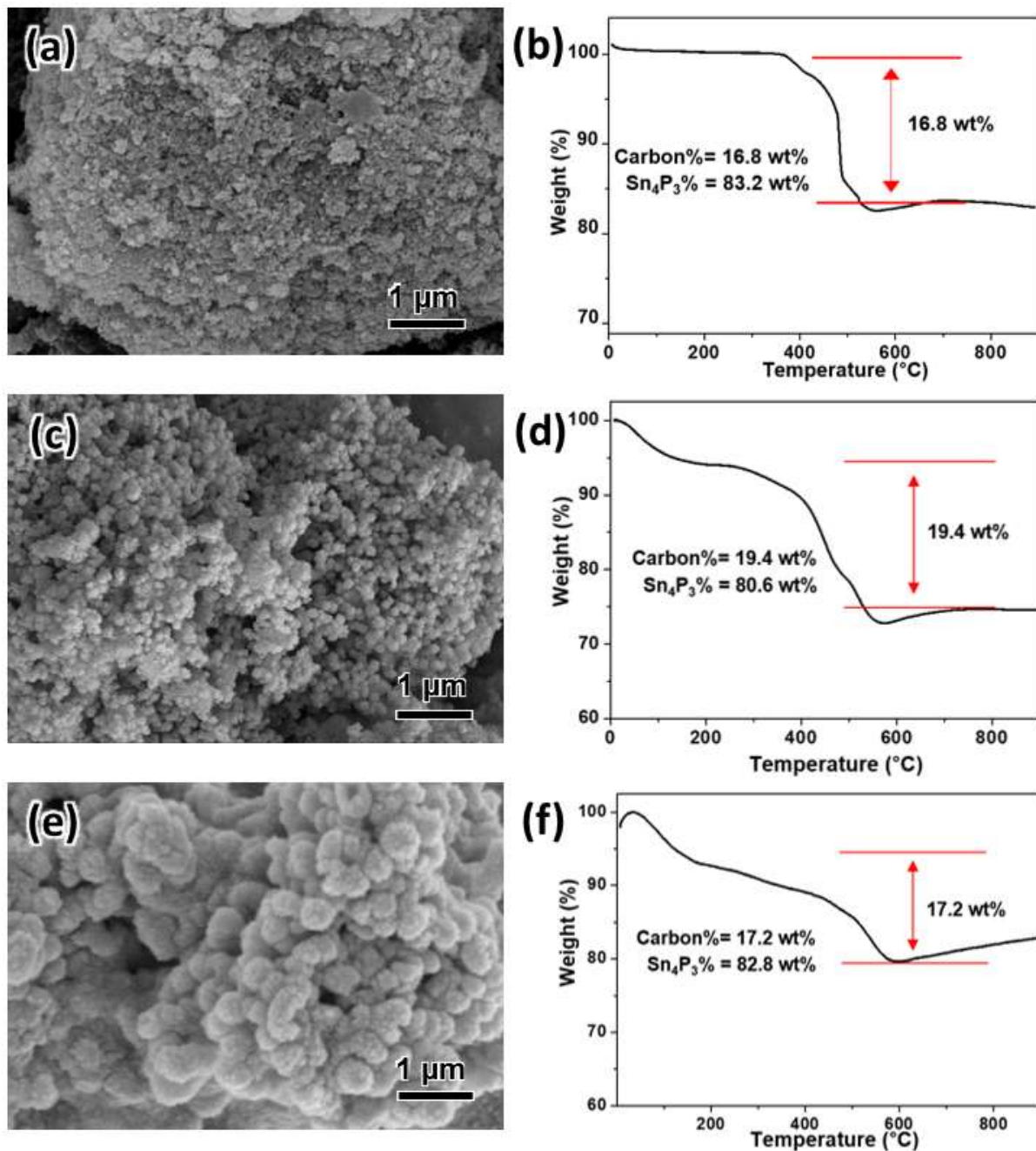


Fig. S4. Low magnification SEM images and TGA curves for Sn_4P_3 -C nanospheres. (a),(b): 30 nm, (c),(d): 140 nm, and (e),(f): 300 nm.

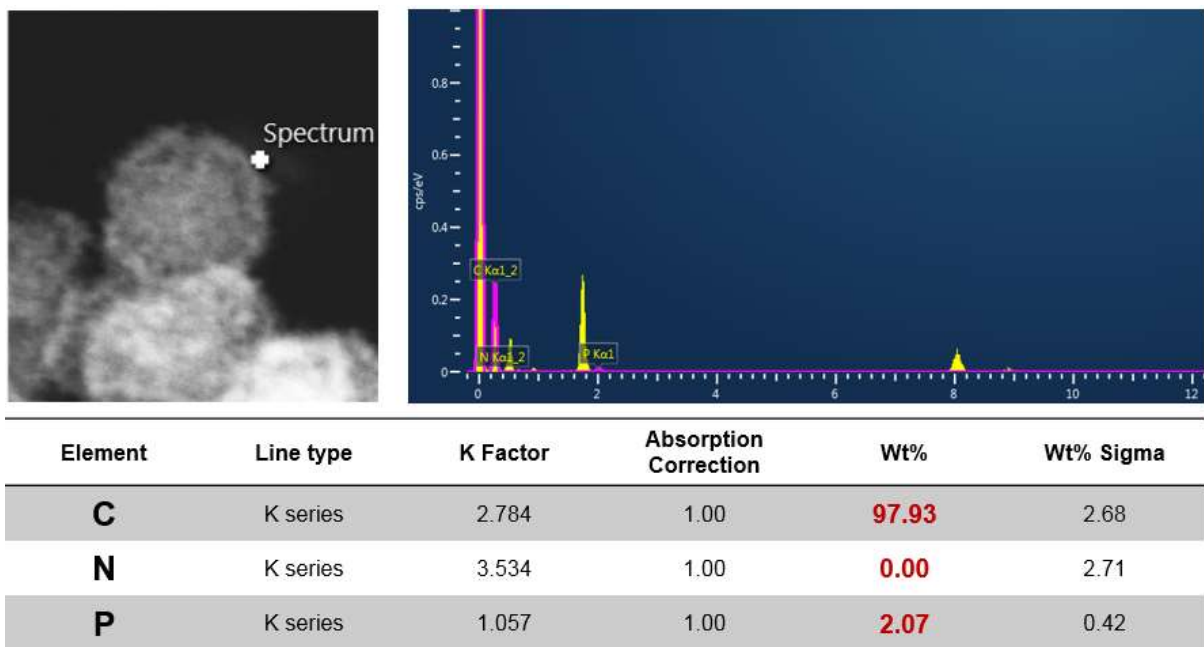


Fig. S5. EDS analysis of carbon shell in $\text{Sn}_4\text{P}_3\text{-C}$ nanospheres.

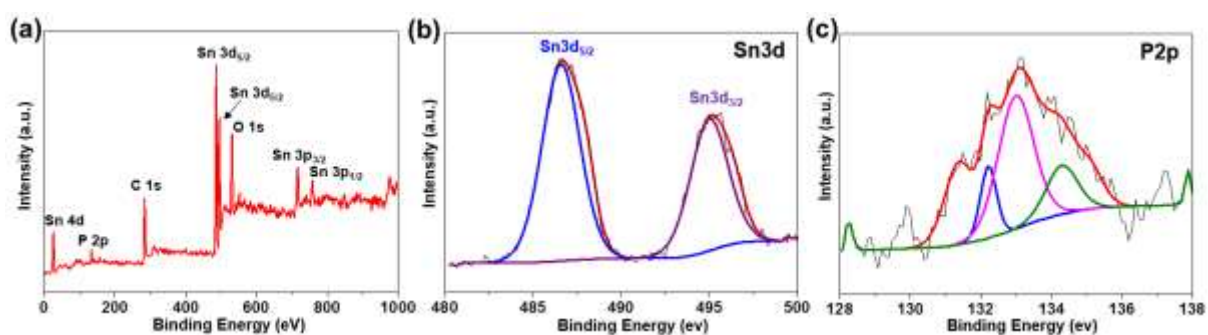


Fig. S6. (A) Survey, (B) Sn3d, and (C) P2p XPS spectra for $\text{Sn}_4\text{P}_3\text{-C}$ nanospheres.

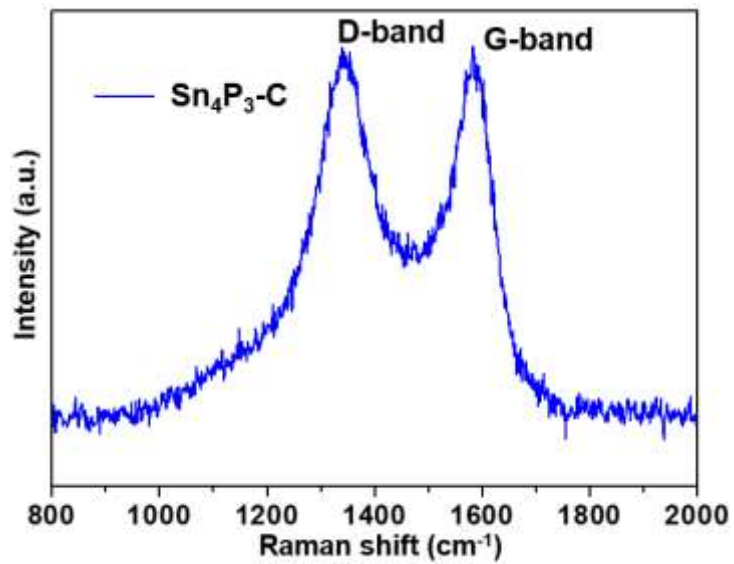


Fig. S7. Raman spectra of synthesized $\text{Sn}_4\text{P}_3\text{-C}$ nanospheres.

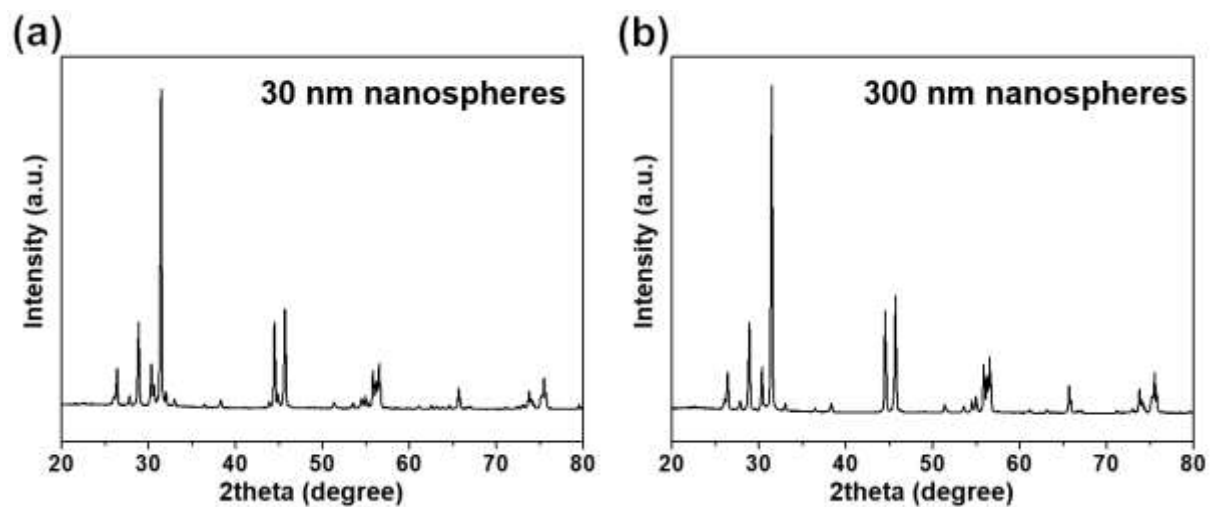


Fig. S8. XRD patterns of (a) 30 nm-sized and (b) 300 nm-sized $\text{Sn}_4\text{P}_3\text{-C}$ nanospheres.

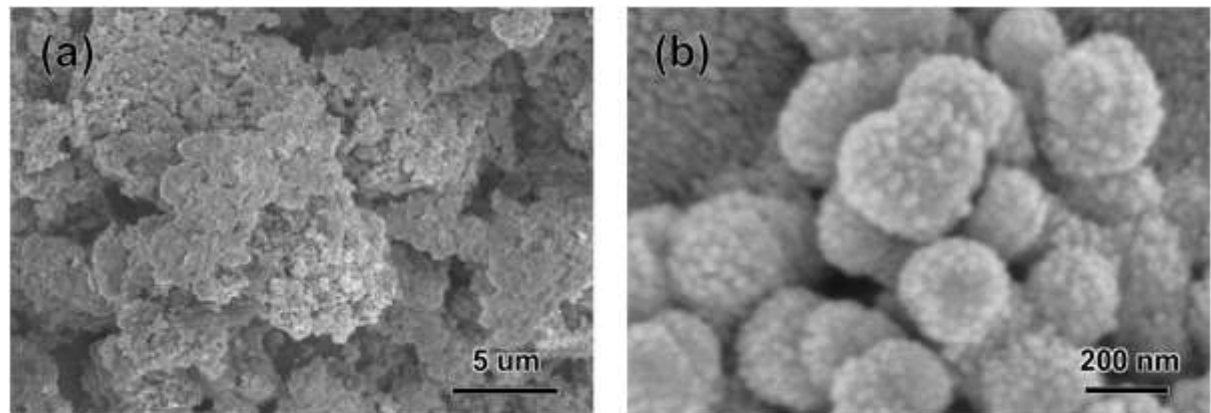


Fig. S9. SEM images of (a) 30 nm-sized nanosphere and (b) 300 nm-sized nanosphere electrodes after 50 cycles at 1000 mA g^{-1} for LIBs.

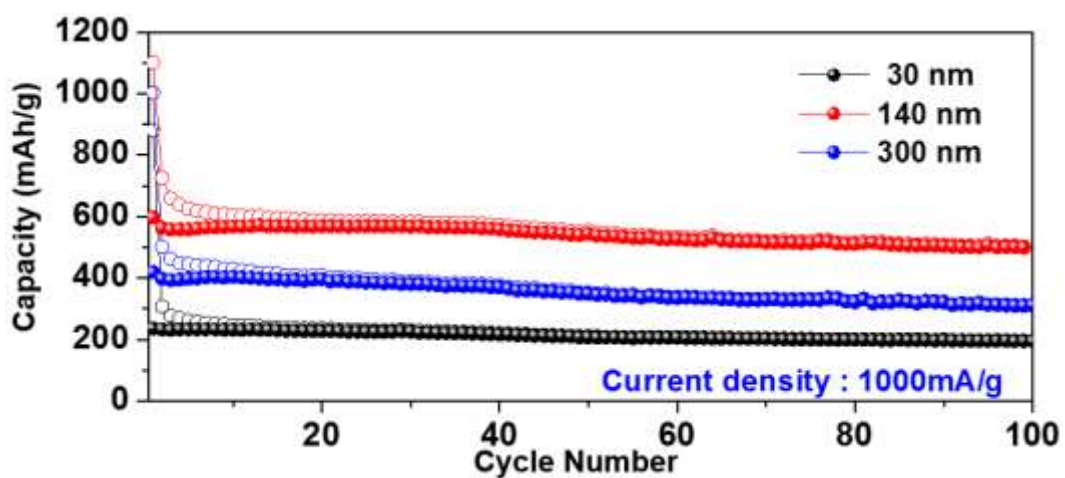


Fig. S10. Cyclability of 30 nm, 140 nm, and 300 nm-sized Sn₄P₃-C nanosphere electrodes at 1000 mA g^{-1} for SIB anode.

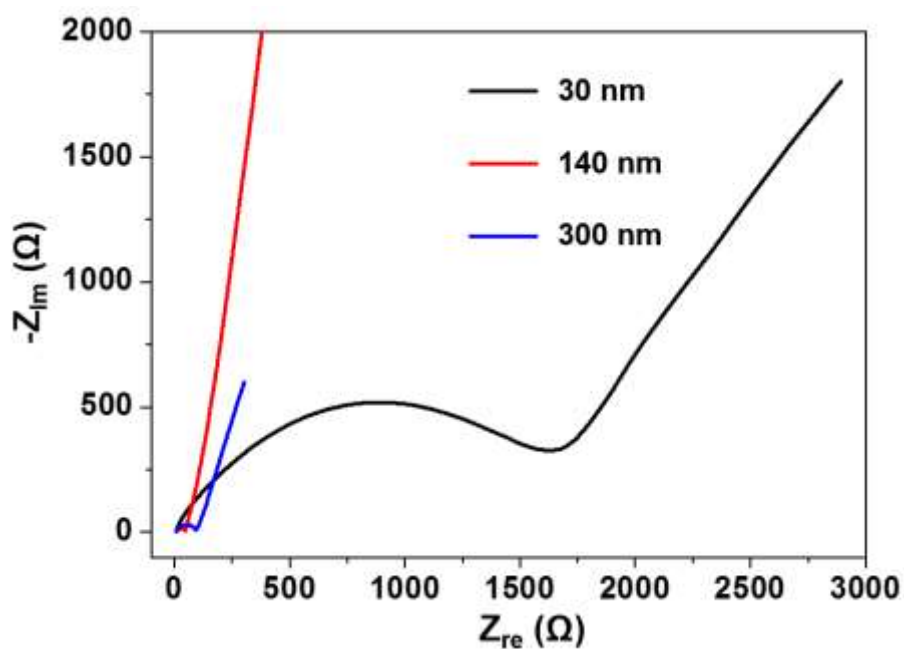


Fig. S11. Electrochemical impedance spectroscopy (EIS) results of 30 nm, 140 nm, and 300 nm-sized Sn₄P₃-C nanosphere electrodes.

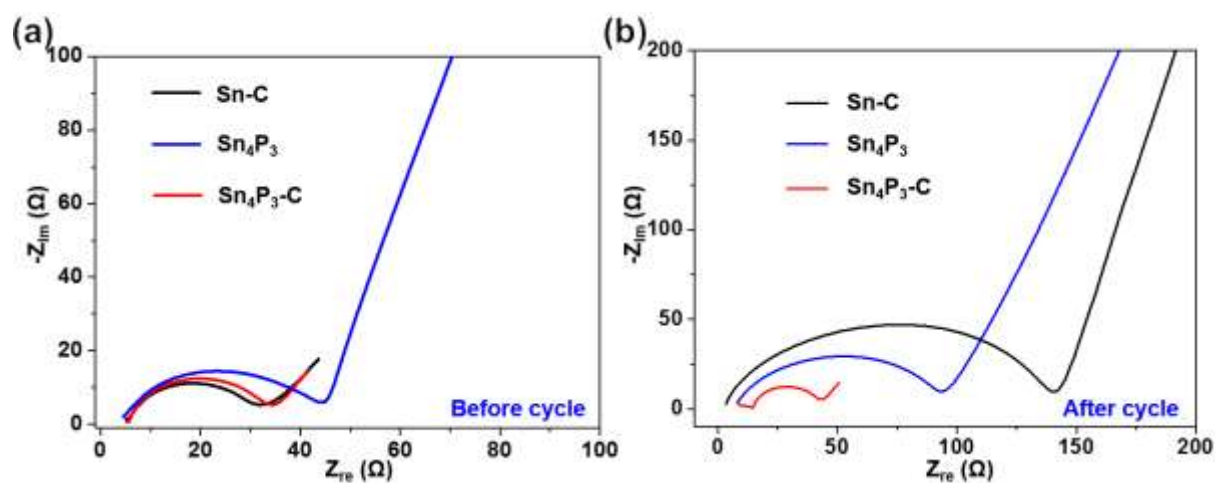


Fig. S12. Electrochemical impedance spectroscopy (EIS) results of Sn-C, Sn₄P₃, and Sn₄P₃-C electrodes (a) before and (b) after 50 cycles.

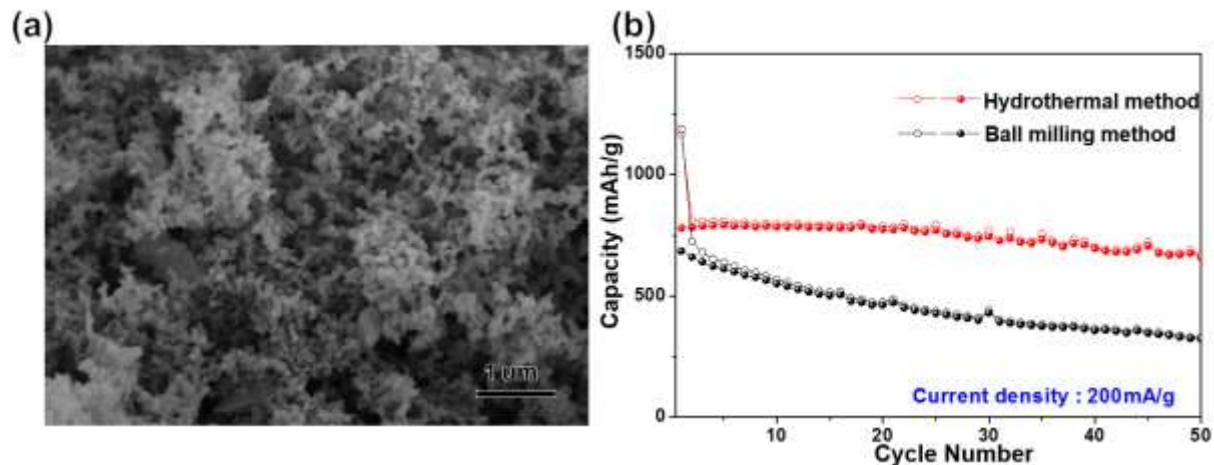


Fig. S13. (a) SEM image of $\text{Sn}_4\text{P}_3/\text{C}$ nanocomposite synthesized by a ball milling method and (b) cyclability of Sn_4P_3 -C nanosphere and $\text{Sn}_4\text{P}_3/\text{C}$ nanocomposite electrode at 200 mA g⁻¹ for SIB anode.

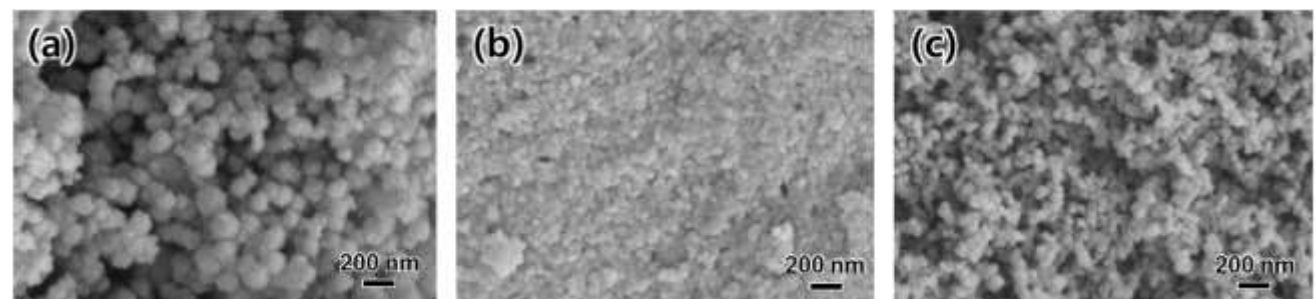


Fig. S14. SEM images of (a) pristine Sn_4P_3 -C nanospheres, (b) cycled Sn_4P_3 -C nanospheres without DMC washing process, and (c) Sn_4P_3 -C nanospheres after DMC washing process.

Table 1. The electrochemical performance of some Sn₄P₃ anode materials for SIB.

Samples	Current density (mA g ⁻¹)	Cycle number	Capacity (mA h g ⁻¹)	Ref.
Sn_{4+x}P₃	100	100	465	[1]
Sn₄P₃-C nanosphere	1500	400	360	[2]
Sn₄P₃	100	50	605	[3]
Sn₄P₃/RGO	1000	1500	362	[4]
Sn₄P₃/C	100	150	500	[5]
Sn₄P₃	100	100	650	[6]
Sn₄P₃	100	320	442	[7]
Sn₄P₃/C	2000	500	368	[8]
Sn₄P₃-P @Graphene	2000	1000	371	[9]
Sn₄P₃-C	2000	2000	420	This work

[1] W. Li, S.-L. Chou, J.-Z. Wang, J. H. Kim, H.-K. Liu and S.-X. Dou, *Adv. Mater.* 2014, 26, 4037-4042.

[2] J. Liu, P. Kopold, C. Wu, P. A. van Aken, J. Maier and Y. Yu, *Energy Environ. Sci.* 2015, 8, 3531-3538.

[3] J. Y. Jang, Y. Lee, Y. Kim, J. Lee, S.-M. Lee, K. T. Lee, and N.-S. Choi, *J. Mater. Chem. A*, 2015, 3, 8332-8338.

[4] Q. Li, Z. Li, Z. Zhang, C. Li, J. Ma, C. Wang, X. Ge, S. Dong and L. Yin, *Adv. Energy Mater.* 2016, 6, 1600376.

[5] J. Qian, Y. Xiong, Y. Cao, X. Ai and H. Yang, *Nano Lett.* 2014, 14, 1865-1869.

[6] Y. Kim, Y. Kim, A. Choi, S. Woo, D. Mok, N.-S. Choi, Y. S. Jung, J. H. Ryu, S. M. Oh and K. T. Lee, *Adv. Mater.* 2014, 26, 4139-4144.

- [7] S. Liu, H. Zhang, L. Xu, L. Ma and X. Chen, *J. Power Sources*, 2016, 304, 346-353.
- [8] L. Ma, P. Yan, S. Wu, G. Zhu and Y. Shen, *J. Mater. Chem. A*, 2017, 5, 16994-17000.
- [9] Y. Xu, B. Peng and F. M. Mulder, *Adv. Energy Mater.* 2018, 8, 1701847.